

# Proton-Conducting Composite Membranes Based on Sulfonated Poly(ether sulfone) and Surface-Modified Tin Phosphate

Shoichi Sugata<sup>\*1</sup>, Shinya Suzuki<sup>2</sup>, Masaru Miyayama<sup>3</sup>

<sup>1, 2, 3</sup>School of Engineering, The University of Tokyo, 7-3-1 Hongo, Bunkyo-ku, Tokyo 113-8656, Japan

<sup>3</sup>CREST, JST, 4-8-1 Honcho, Kawaguchi, Saitama 332-0012, Japan

<sup>\*1</sup>sugata@fmat.t.u-tokyo.ac.jp; <sup>3</sup>miyayama@fmat.t.u-tokyo.ac.jp

**Abstract**-Organic/inorganic composite membranes were prepared by dispersing *m*-sulfophenyl-group-modified layered tin phosphate hydrate particles (SnPP-SPP) or nanosheets (SnPNS-SPP) in sulfonated poly(ether sulfone) (SPES). The chemical stabilities, as evaluated by Fourier-transform infrared spectroscopy and water-uptake measurements, were improved by dispersion of SnPP-SPP or SnPNS-SPP into the SPES matrix. The proton-conducting properties of the composite membranes were improved by the sulfophenyl group modification; among the composite membranes, the membrane containing 10 vol% SnPNS-SPP showed the highest conductivity of  $8.0 \times 10^{-2} \text{ S cm}^{-1}$  at 150 °C under saturated water-vapor pressure.

**Keywords**- Organic/Inorganic Nanocomposite; Proton Conductors; Fuel Cell

## I. INTRODUCTION

Fuel cells have received increasing attention as high-efficiency systems for energy conversion. Of the various fuel cells, the proton-exchange membrane fuel cell (PEMFC) is considered to be the most promising as a source of power for a wide range of applications. However, the PEMFC suffers from a number of problems such as poisoning of the platinum-based catalyst by carbon monoxide, a decrease in the effective area of the electrodes as a result of the adsorption of liquid water, and difficulties in heat exchange. To overcome these problems, the operation of fuel cells at intermediate temperatures above 100 °C is a promising method [1]. However, polymer membranes generally show insufficient heat resistance to permit long-term use at such temperatures, and their proton conductivity is reduced as a result of dehydration under conditions of low relative humidity (RH) at intermediate temperatures [2, 3]. It would therefore be desirable to develop polymer electrolyte membranes (PEMs) that combine a high proton conductivity ( $\sigma > 10^{-2} \text{ S cm}^{-1}$ ) with an enhanced chemical stability at intermediate temperatures [2, 4-6].

Because of their thermal stability, hydrocarbon polymers have frequently been used as PEMs at intermediate temperatures. In attempts to improve the thermal stability and dry durability of such membranes, many studies have been conducted on the addition of inorganic compounds to heat-resistant organic matrices such as sulfonated poly(ether ether ketone) (SPEEK) or sulfonated poly(ether sulfone) (SPES) [7-14]. Reduced permeation of reaction gases, reduced swelling, enhanced mechanical properties, and improved conductivities have been achieved with some composite systems, such as SPEEK/WO<sub>3</sub>, SPES/heteropoly acid (H<sub>3</sub>PW<sub>12</sub>O<sub>40</sub>), SPES/boron phosphate (BPO<sub>4</sub>), and SPEEK/organically-treated montmorillonite [9, 10, 15-20]. It has also been reported that protons transfer rapidly through the interface between the two materials in some proton-conducting organic/inorganic composites [10, 21].

Layered metal(IV) hydrogen phosphates  $\text{M}(\text{HPO}_4)_2 \cdot n\text{H}_2\text{O}$  are proton-conducting materials that contain water molecules in interlayers [22, 23]. In particular,  $\text{Sn}(\text{HPO}_4)_2 \cdot n\text{H}_2\text{O}$  (SnP), which consists of primary  $\text{Sn}(\text{HPO}_4)_2$  layers and interlayer water molecules, shows a high and stable proton conductivity above 100 °C [23]. SPEEK/SnP and SPES/SnP composite membranes show good thermal stabilities and proton conductivities at temperatures of up to 150 °C [24, 25]. Some layered inorganic compounds can be exfoliated to form nanosheets (NS) that have larger specific surface areas than the corresponding particulate inorganic compounds [26-29]. Composite membranes containing inorganic nanosheets should therefore have much larger organic-inorganic interfacial areas than the corresponding composites containing inorganic particles. Because of the surface properties of TiO<sub>2</sub>-NS/SPEEK, composites with low TiO<sub>2</sub>-NS contents have higher proton conductivities than that of pure SPEEK [30]. It has also been reported that the large area of the SPEEK-Zr(HPO<sub>4</sub>)<sub>2</sub> · nH<sub>2</sub>O-NS ( $\alpha$ -ZrP-NS) interface results in improvements in the proton conductivity of the composites at intermediate temperatures and greater resistance to drying [31]. In our previous report, it has reported that the effects of structural stabilization and the conductivity improvement were more evident for SPES/SnPNS membranes than for SnP particle-containing SPES (SPES/SnPP) membranes [32]. It was concluded that the larger interfacial area of SPES/SnPNS membranes leads to improved chemical stability and enhanced proton conductivity compared with SPES/SnPP membranes, and that the connectivity of the SPES-SnP interfacial layer operates effectively as a proton-conducting path.

In relation to the modification of metal phosphates,  $\gamma$ -zirconium phosphate phenylphosphonate  $\{\text{ZrPO}_4(\text{H}_2\text{PO}_4)_{1-x}[\text{P}(\text{O}_2)\text{Ph}]_x\}$  can be prepared by a topotactic reaction between  $\gamma$ -zirconium phosphate  $[\gamma\text{-ZrPO}_4(\text{H}_2\text{PO}_4) \cdot 2\text{H}_2\text{O}]$

and a solution of phenylphosphonic acid [33-35]. The phosphate groups in  $\alpha$ -zirconium phosphate can be partially replaced by *m*-sulfophenylphosphonate (SPP) groups [36, 37]. The conductivity of the resulting zirconium phosphate sulfophenylphosphonate (ZrPSPP) is comparable with that of Nafion, and the layered structure of the phosphate is not changed by the replacement [38, 39]. Therefore, sulfophenyl group-modified metal phosphates might be suitable fillers for increasing the proton conductivity of low-conductivity polymers. However, sulfophenyl group modification (SPP-modification) of the SnP surface has not previously been reported.

In the present study, composite membranes of SPES/SPP-modified SnP particles (SnPP-SPP) and SPES/SPP-modified SnP nanosheets (SnPNS-SPP) were prepared and their chemical stabilities and their proton conductivities at intermediate temperatures were examined.

## II. EXPERIMENTAL

SPES was prepared by direct aromatic nucleophilic substitution stepwise polymerization, as reported earlier [40,41]. The average number of sulfonic acid groups per repeat unit of SPES polymer (the degree of sulfonation) was evaluated by titration to be 1.0.

The SnP particles (SnPP) were synthesized by a hydrothermal reaction as described elsewhere [23]. The SnP nanosheets (SnPNS) were prepared through intercalation-exfoliation of SnPP, as reported earlier, [31, 32] and dispersed in *N,N*-dimethylacetamide (DMA; Wako Pure Chemical Industries).

The exchange of phosphate groups of SnP for sulfophenylphosphonate groups was examined by dispersing SnP in an aqueous solution of 3-phosphonobenzenesulfonic acid [3-(HO)<sub>2</sub>P(O)C<sub>6</sub>H<sub>4</sub>SO<sub>3</sub>H; H<sub>2</sub>SPP] and heating under reflux. A similar procedure for the exchange reaction has been described in earlier reports [34, 35]. H<sub>2</sub>SPP was synthesized by the method of Montoneri *et al* [42]. SnPP or SnPNS (1 g) were dispersed in 1 M aqueous H<sub>2</sub>SPP (100 mL), and the mixture was refluxed for 24 hours. The exchanged product (SnP-SPP) was separated by centrifugation and washed repeatedly with deionized water to remove residual H<sub>2</sub>SPP then dispersed in deionized water by agitation. The concentrations of Sn and P in the dispersion were measured by inductively coupled plasma atomic-emission spectroscopy (ICP-AES) on an SPS3100 instrument (SII Nanotechnology Inc., Chiba).

Composite membranes of SPES and SnP (SnPP, SnPNS SnPP-SPP, and SnPNS-SPP) were prepared by solution casting of mixtures of SPES with SnP at various volume ratios from 0 to 30 vol% SnP. SnP was dispersed in DMA and ultrasonicated for 24 hours. The appropriate amount of SPES was then dissolved in the DMA suspension of SnP. After mixing and defoaming in a conditioning mixer (ARE250; Thinky, Tokyo), the resulting mixture was cast onto a Teflon plate and kept at 80 °C overnight. The membranes that formed were immersed in 1 M H<sub>2</sub>SO<sub>4</sub> for 24 hours, washed with deionized water, and finally dried at 80 °C for 48 hours in air. The thickness of the resulting membranes was 150–300 μm. The crystal structures of SPES/SnPP-SPP and SPES/SnPNS-SPP were determined by X-ray diffraction (XRD) using Cu K $\alpha$  radiation (Bruker AXS) at room temperature.

Thermogravimetric analysis (TGA) and differential thermal analysis (DTA) were performed with a Thermoplus TG8120 (Rigaku, Tokyo) at a heating rate of 10 °C/min under dry air.

Fourier-transform infrared (FT-IR) spectra of the prepared membranes were recorded at room temperature on an IR Prestage-21 spectrometer (Shimadzu, Kyoto); the spectra were obtained as averages of 100 scans with a resolution of 2 cm<sup>-1</sup>. Raman spectra were recorded on a Jasco NR-1000 spectrometer with excitation at 532.36 nm by a JUNO 100 green laser (Showa Optronics Co., Ltd, Tokyo).

The water uptake (*WU*) of the prepared membranes as a mass percentage was estimated by using the following equation:

$$WU \text{ (wt\%)} = [(W_{\text{wet}} / W_{\text{dry}}) - 1] \times 100$$

where  $W_{\text{wet}}$  is the weight of the wet membrane and  $W_{\text{dry}}$  is the weight of the dry membrane. The weight of the wet membrane was determined by immersing the dry membrane in water at 30 °C for 48 hours, wiping off surface water with absorbent paper, and weighing.

The conductivity was measured by the impedance method over the frequency range 5 Hz to 13 MHz at an applied voltage of 0.1 V by using a 4192A impedance analyzer (Hewlett Packard, Palo Alto, CA). Silver electrodes were attached to the surface of membranes by painting them on as a paste and drying at 60 °C. The samples were placed in a stainless vessel at 40–150 °C under saturated water vapor pressure.

## III. RESULTS AND DISCUSSION

Fig. 1 shows the XRD patterns of the SPES/SnPP, SPES/SnPNS, SPES/SnPP-SPP and SPES/SnPNS-SPP composite membranes. The main diffraction peaks of both samples can be indexed to the orthorhombic phase of Sn(HPO<sub>4</sub>)<sub>2</sub> · H<sub>2</sub>O (JCPDS Card No. 31-1397); the peaks at 22° and 29° are attributed to the clay used to hold the sample. The diffraction peak at about

10°, attributed to (006), did not shift after the exchange reaction and the interlayer distance of SnP was unchanged, suggesting that H<sub>2</sub>SPP is exchanged with phosphate groups at the SnP surface but not inserted into interlayers.

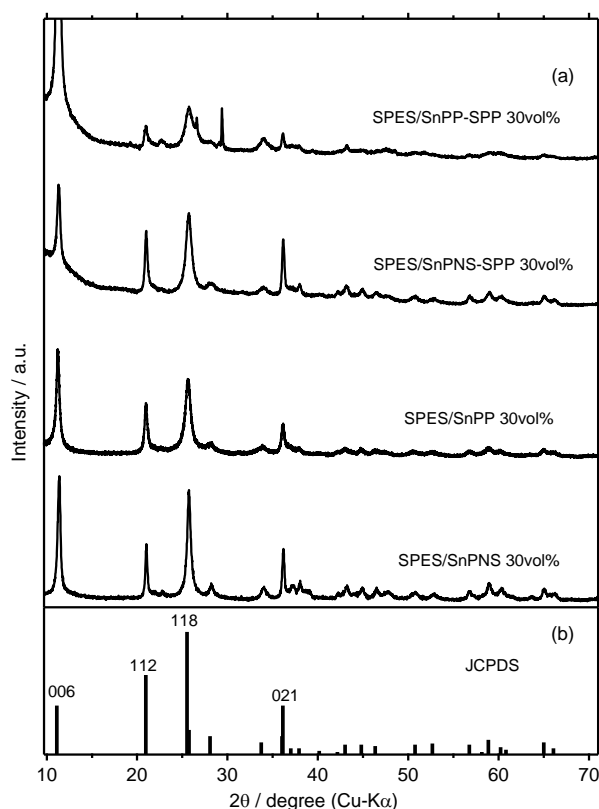


Fig. 1 (a) XRD patterns of composite membranes containing 30 vol% SnP, SnPNS, SnPP-SPP or SnPNS-SPP, and (b) the peak assignment in JCPDS 31-1397 for Sn(HPO<sub>4</sub>)<sub>2</sub>·H<sub>2</sub>O

The atomic ratios of sulfur in sulfophenylphosphonate groups to phosphorus in total phosphate groups in SnPP-SPP and SnPNS-SPP, as measured by ICP-AES, were 1:90 and 1:16, respectively. This confirmed that sulfur was introduced into SnP-SPP by the exchange reaction. Fig. 2 shows the Raman spectra for SnPP and SnPP-SPP. The peak at 1130 cm<sup>-1</sup> for SnPP-SPP was assigned to the ν(SO<sub>2</sub>) mode of the SO<sub>3</sub>H group [43,44]. It is thought that the SO<sub>3</sub>H groups are present on the surface of SnPNS-SPP, because H<sub>2</sub>SPP is not intercalated into SnP, as indicated in Fig. 1. It is therefore likely that the exchange reaction between SnP and H<sub>2</sub>SPP (SPP-modification) occurs on the surface of the SnP and the reaction is as follows:

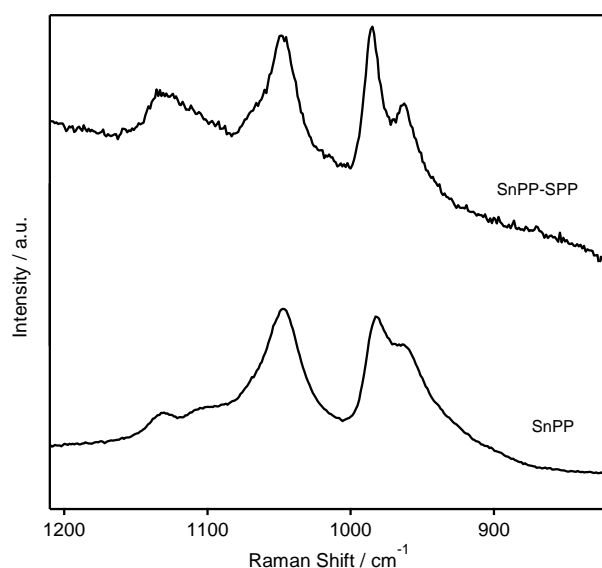
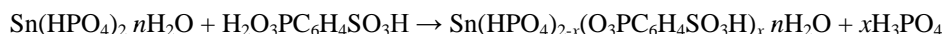


Fig. 2 Raman spectra of SnPP and SnPP-SPP

Schematic illustrations of the structures of H<sub>2</sub>SPP and SnP-SPP are presented in Fig. 3.

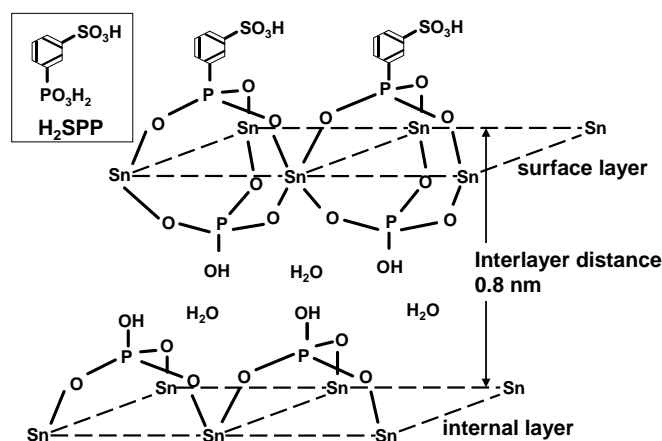


Fig. 3 Schematic showing the structures of H<sub>2</sub>SPP and Sn(HPO<sub>4</sub>)<sub>2-x</sub>(O<sub>3</sub>PC<sub>6</sub>H<sub>4</sub>SO<sub>3</sub>H)<sub>x</sub> · nH<sub>2</sub>O

Fig. 4 shows an image of SnPNS-SPP deposited on a mica substrate recorded by atomic force microscopy (AFM). The thickness and the lateral size of the SnPNS-SPP samples were 6–9 nm and 50–100 nm, respectively. The thickness of the unmodified SnPNS is 1–5 nm [32]. The change in thickness of the modified sheet suggests that the SnP nanosheets were partly restacked during the exchange reaction. The interlayer distance of SnP is 0.8 nm; the thickness of the SnPNS-SPP layer therefore corresponds to 8–10 primary Sn(HPO<sub>4</sub>)<sub>2</sub> layers. Provided the exchange reaction occurs only at the SnP surface, as described above, if all the phosphate groups present on the surface were exchanged by sulfophenyl groups, the ratio of exchanged phosphate groups to total phosphate groups would be between 1:8 and 1:10. However the actual S-to-P concentration ratios in SnPNS-SPP measured by ICP-AES were 1:16. Therefore, we can estimate that about half the surface phosphate groups of SnPNS were exchanged by *m*-sulfophenylphosphonic groups. The exchange ratio of the surface phosphate groups of SnP particles by the same method was examined, and it was found that the estimated ratio was also about half.

SnPNS was obtained by the delamination of SnPP and a little SnP nanosheets re-stacked probably during the exchange reaction. The sulfophenyl groups are present on the surface of the nanosheets and particles. In our previous report, partly re-stacked nanosheets did not sink into the bottom of the composite membrane and they were dispersed in a similar level to the SPES/SnPP composite membrane [32]. It is considered that SnPNS-SPP dispersed in SPES as well.

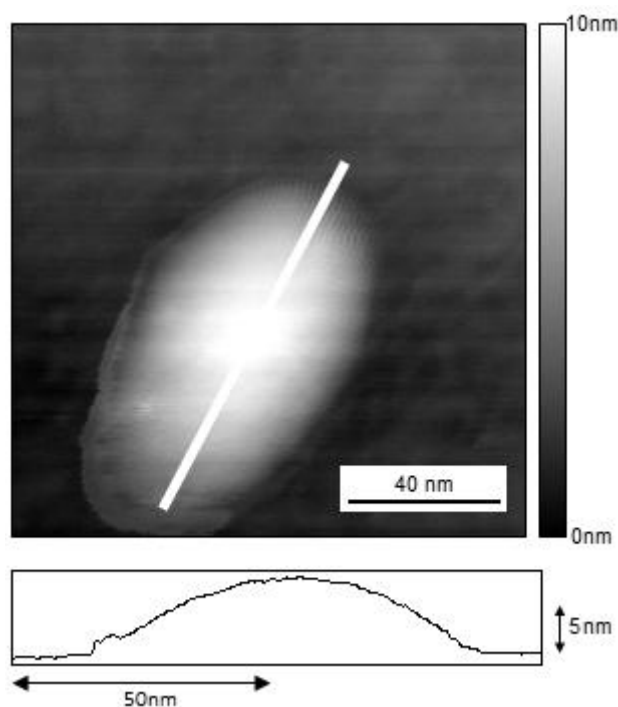


Fig. 4 AFM images of SnPNS-SPP. The upper image is a two-dimensional diagram, and the lower image shows a cross-sectional diagram at the white line that appears in the upper image

Fig. 5 shows the water uptake of the SPES/SnP, SPES/SnPNS, SPES/SnP-SPP and SPES/SnPNS-SPP membranes. The water uptake decreased with increasing SnP content in all composites. On addition of 40 vol% of SnP, the water uptakes of membranes became about half of that of pure SPES, leading to the suppression of swelling. The decrease in water uptake of the SPES/SnP composite membranes is the result of stabilization of the microstructure (i.e., suppression of excessive swelling) by the hydrogen-bond network at the SPES–SnP interface, as reported for SPEEK/SnP composite membranes [31]. The degree of decrease of water uptake in the SPES/SnPNS membranes was greater than that in SPES/SnP membranes [32], whereas the degree of decrease of water uptake in SPES/SnPNS-SPP membranes was smaller than that in SPES/SnP-SPP membranes. It is likely that the amount of water in the SPES–SnPNS-SPP interface is larger than that in the SPES–SnPNS interface because of the higher concentration of  $\text{SO}_3\text{H}$  groups at the interface. The water uptake of the composite membranes containing 0 vol% unmodified SnP was smaller than that of the composite membranes containing 0 vol% SPP-modified SnP. This is because the used SPES were different and the concentrations of sulfone groups in SPES were different in ref. 32. All the composite membranes with SPP-modified SnP were prepared by using the same polymer. The concentrations of sulfone groups in SPES of all SPES/SnPNS-SPP and SPES/SnP-SPP composite membranes are the same.

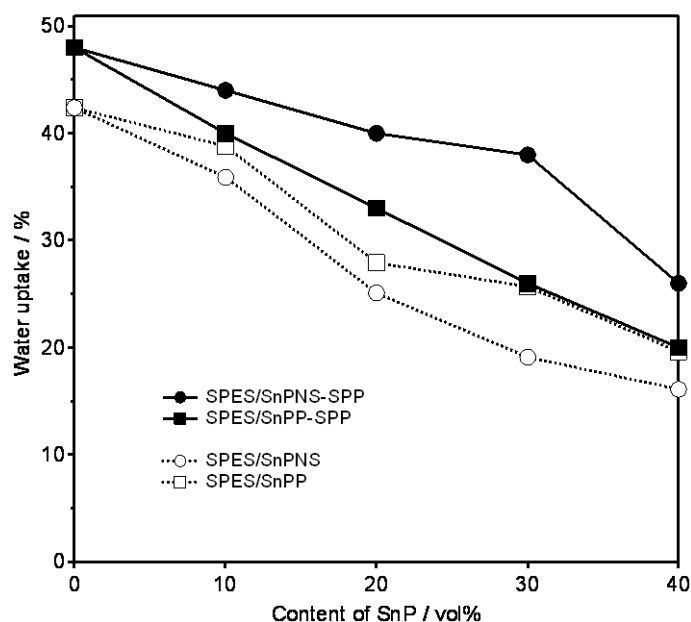


Fig. 5 Water uptakes of SPES/SnP-SPP membranes with various SnP contents. Water uptakes of SPES/SnP membranes were also plotted [32]

In the FT-IR spectra of the membranes (not shown), a peak attributed to the symmetric  $\text{SO}_3^-$  stretching vibrations of the sulfonate group appeared at around  $1030\text{ cm}^{-1}$  [45]. Fig. 6 shows the dependence of the position of this peak on the SnP content for SPES/SnP, SPES/SnPNS, SPES/SnP-SPP and SPES/SnPNS-SPP membranes. The wavenumbers for the peaks for all membranes increased with increasing SnP content. Shifting of sulfonic acid vibrations to higher values indicates strong hydrogen-bonding interactions and structural stabilization [45]. It is suggested that composite membranes contain stronger hydrogen bonds than does pure SPES membrane and that the presence of a hydrogen-bond network at the SPES–SnP-SPP interface improves the structural stability, as reported previously [24, 25, 32]. The peak shift for SPES/SnPNS-SPP membranes was larger than that for SPES/SnP-SPP membranes, indicating that the effect of stabilization was increased by enlargement of the SPES–SnP-SPP interfacial area. The extent of the shifts of the peaks for SPES/SnPNS-SPP was almost as same as that for SPES/SnPNS(unmodified) [32]. Therefore it is suggested that hydrogen-bond networks are formed by SPP-modified SnP addition as strongly as at unmodified SnP addition.

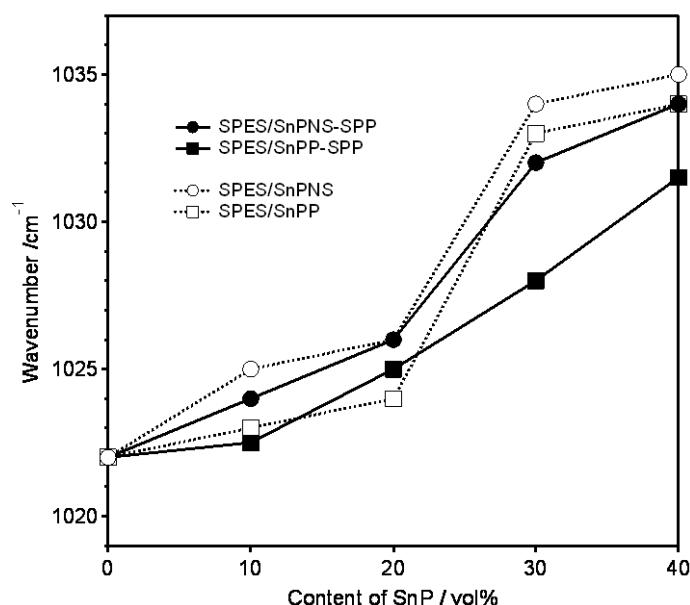


Fig. 6 Wavenumbers of the  $\text{SO}_3^-$  bands in the FT-IR spectra of SPES/SnP-SPP membranes. Wavenumbers for SPES/SnP membranes were also plotted [32]

Fig. 7 shows the dependence of the splitting-off temperature on the SnP content for SPES/SnPNS and SPES/SnPNS-SPP membranes as measured by TGA. Several weight-loss steps were observed from TG curves (not shown here). On the basis of previous studies on SPEEK-based membranes [10,12], we attributed the weight losses at 290–310 °C to the elimination of the  $\text{SO}_3\text{H}$  groups from SPES chain, and we defined the temperature as the splitting-off temperature ( $T_s$ ) hereafter.  $T_s$  of both membranes increased with increasing SnP content. It has been reported that organic/inorganic composite structures are stabilized by hydrogen bonds formed between  $\text{SO}_3\text{H}$  groups in a sulfonated polymer and interlayer water of a layered inorganic compound [10, 45]. It can be concluded that the presence of a network of hydrogen bonds at the SPES–SnP interface improves the thermal stability.

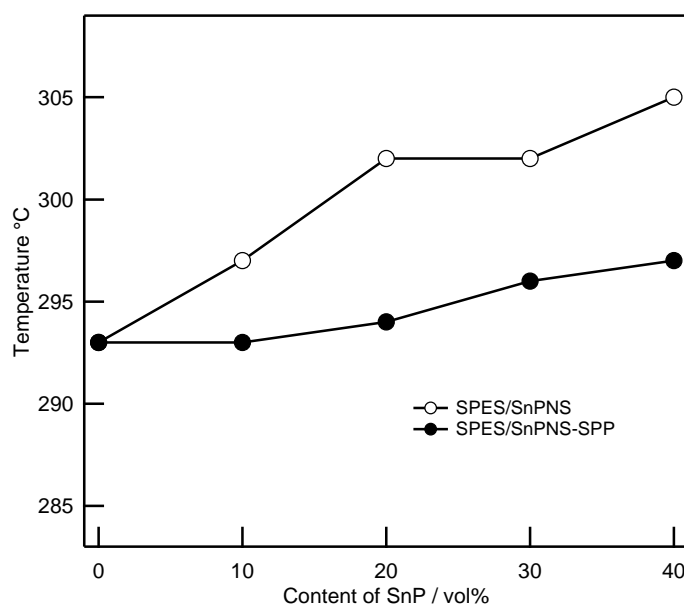


Fig. 7 Splitting-off temperatures of  $\text{SO}_3\text{H}$  groups for SPES/SnPNS and SPES/SnPNS-SPP membranes

Fig. 8 shows the temperature dependence of the conductivities of pure SPES and the composite membranes containing 10 vol% SnP particles (SPES/SnP10vol%), 10 vol% SnP nanosheets (SPES/SnPNS10vol%), 10 vol% SPP-modified SnP particles (SPES/SnP-SPP10vol%), and 10 vol% SPP-modified SnP nanosheets (SPES/SnPNS-SPP10vol%) measured under saturated water vapor pressure. The SPES/SnPNS-SPP10vol% membrane showed the highest conductivity among the membranes measured, and the conductivity at 150 °C was  $8.0 \times 10^{-2} \text{ S cm}^{-1}$ . The SPES/SnP-SPP10vol% membrane showed a higher conductivity than SPES/SnP10vol% at below 100 °C. The conductivities of composite membranes were improved by SPP-modification. However the degree of the improvement in SPES/SnP-SPP10vol% by SPP-modification was smaller than that in SPES/SnPNS-SPP10vol%. The conductivity of SPES/SnP10vol% was slightly lower than those of pure SPES. Because of the small interfacial area of the SPES–SnPP, the hydrogen-bond network is probably intermittently connected in

SPES/SnPP10vol% as described in ref.32. It is thought that the effect of the improvement by SPP-modification of SnPP was hard to be seen for the same reason.

SPES/SnPNS-SPP10vol% membrane showed the highest conductivity, and the conductivity for SPES/SnPNS-SPP composite membranes decreased with increasing SnPNS-SPP content above 20 vol% (not shown here). That is consistent with our previous results (ref. 32) for the conductivity dependence of SPES/SnPNS composite membranes. This is because of a decrease in water content accompanied with structural stabilization by SnPNS-SPP addition. The slopes of conductivity plots for all samples became steeper above 100 °C. Usually, the activation energy depends on the water content in the electrolyte and the activation energy decreases with increasing water content [46]. The steep slope above 100 °C is assumed to be in the state of high activation energy with a low water content.

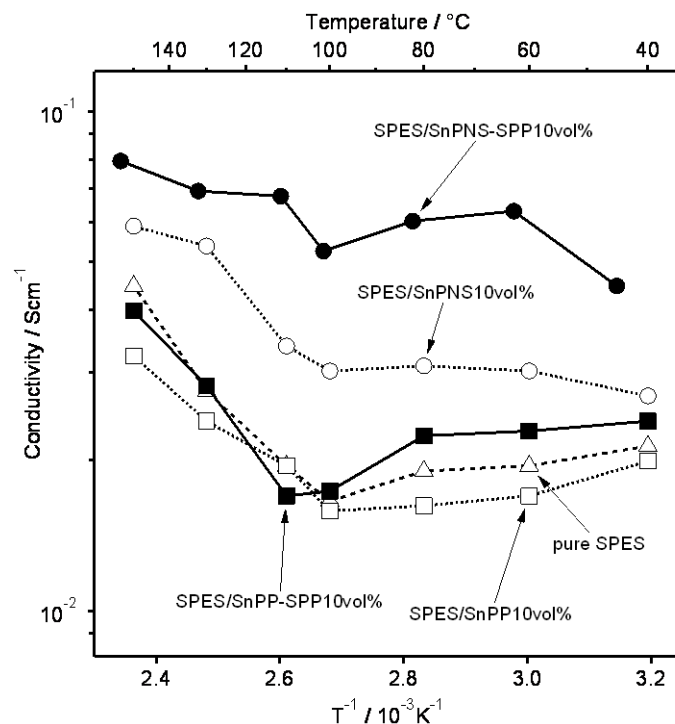


Fig. 8 Temperature dependence of the conductivity of pure SPES and the composite membranes containing 10 vol% SnPP, SnPNS, SnPP-SPP and SnPNS-SPP at saturated water vapor pressure

In our previous report, the proton-conducting properties of composite membranes were improved by the addition of SnP to an SPES matrix and that the degree of improvement in the conductivity of SPES/SnPNS membranes was larger than that for SPES/SnPP [32]. It was concluded that the formation of a hydrogen-bond network permits protons to transfer rapidly by hopping through the network. It was also concluded that the use of SnP nanosheets is more effective in increasing the organic-inorganic interfacial area and the connectivity of the SPES-SnP interfacial layer, which operates effectively as a proton-conducting path. The results shown in Fig. 8 are consistent with our previous results, and the conductivity of the membrane containing SnP nanosheets (SPES/SnPNS-SPP10vol%) was greater than that of the membrane containing SnP particles (SPES/SnPP-SPP10vol%). Furthermore, the conductivity of the SPES/SnPNS-SPP10vol% membrane was higher than that of the SPES/SnPNS10vol% membrane, even though the interfacial area of SPES-SnPNS-SPP was smaller than that of SPES-SnPNS, as evaluated by AFM measurements. This indicates that the conductivity of the organic-inorganic interface is improved by sulfophenyl group modification of the SnP surface with H<sub>2</sub>SPP, leading to a higher concentration of SO<sub>3</sub>H groups at the interface.

#### IV. CONCLUSIONS

SPES/SnP-SPP membranes with various volume ratios of SnP-SPP to the SPES matrix (0–30 vol%) were prepared and characterized. Sulfophenyl group modification of the SnP surface was accomplished by exchange reaction of phosphate groups on the SnP surface with *m*-sulfophenylphosphonic acid. FT-IR and the water-uptake measurements showed that hydrogen-bond networks are formed between SPES and SnP-SPP in the composite membranes. The formation of the hydrogen-bond networks leads to the structural stabilization of the composite membranes. The proton-conducting properties of composite membranes were also improved by the sulfophenyl group modification of the SnP surface. This improvement is probably due to the high concentration of sulfonic acid groups at the organic-inorganic interface. The degree of improvement in the conductivity of SPES/SnPNS-SPP membranes was greater than that for SPES/SnPP-SPP. It is confirmed that the conductivity was improved by increasing the SPES-SnP interfacial area, which operates effectively as a proton-conducting path. Among the

prepared composite membranes, the membrane containing 10 vol% SnPNS-SPP showed the highest conductivity ( $8.0 \times 10^{-2} \text{ S cm}^{-1}$ ) at 150 °C under saturated water vapor pressure.

#### ACKNOWLEDGMENT

The authors are grateful to Toyota Motor Corporation for their support of this research through an entrusted research project.

#### REFERENCES

- [1] Q. Li, R. He, J. O. Jensen, and N. J. Bjerrum, "Approaches and recent development of polymer electrolyte membranes for fuel cells operating above 100 °C," *Chem. Mater.*, vol. 15, pp. 4896-4915, 2003.
- [2] G. Alberti, M. Casciola, L. Massinelli, and B. Bauer, "Polymeric proton conducting membranes for medium temperature fuel cells (110–160°C)," *J. Membr. Sci.*, vol. 185, pp. 73-81, 2001.
- [3] W. H. J. Hogarth, J. C. Diniz da Costa, and G. Q. Lu, "Solid acid membranes for high temperature (140 °C) proton exchange membrane fuel cells," *J. Power Sources*, vol. 142, 223–237, 2005.
- [4] S. Hara, H. Sakamoto, M. Miyayama, and T. Kudo, "Proton-conducting properties of hydrated tin dioxide as an electrolyte for fuel cells at intermediate temperature," *Solid State Ionics*, vol. 154-155, pp. 679-685, 2002.
- [5] N. H. Jalani, K. Dunn, and R. Datta, "Synthesis and characterization of Nafion®-MO<sub>2</sub> (M = Zr, Si, Ti) nanocomposite membranes for higher temperature PEM fuel cells," *Electrochim. Acta*, vol. 51, 553–560, 2005.
- [6] A. Saccà, A. Carbone, E. Passalacqua, A. D'Epifanio, S. Licoccia, et al., "Nafion–TiO<sub>2</sub> hybrid membranes for medium temperature polymer electrolyte fuel cells (PEFCs)," *J. Power Sources*, vol. 152, pp. 16-21, 2005.
- [7] M. L. Di Vona, A. D'Epifanio, D. Marani, M. Trombetta, E. Traversa, and S. Licoccia, "SPEEK/PPSU-based organic–inorganic membranes: Proton conducting electrolytes in anhydrous and wet environments," *J. Membr. Sci.*, vol. 279, pp. 186-191, 2006.
- [8] M. L. Hill, Y. S. Kim, B. R. Einsla, and J. E. McGrath, "Zirconium hydrogen phosphate/disulfonated poly(arylene ether sulfone) copolymer composite membranes for proton exchange membrane fuel cells," *J. Membr. Sci.*, vol. 283, pp. 102-108, 2006.
- [9] S. Licoccia and E. Traversa, "Increasing the operation temperature of polymer electrolyte membranes for fuel cells: From nanocomposites to hybrids," *J. Power Sources*, vol. 159, pp. 12-20, 2006.
- [10] B. Mecheri, A. D'Epifanio, M. L. Di Vona, E. Traversa, S. Licoccia, and M. Miyayama, "Sulfonated polyether ether ketone-based composite membranes doped with a tungsten-based inorganic proton conductor for fuel cell applications," *J. Electrochem. Soc.*, vol. 153, pp. A463-A467, 2006.
- [11] J.-M. Thomassin, C. Pagnoulle, D. Bizzari, G. Caldarella, A. Germain, and R. Jérôme, "Improvement of the barrier properties of Nafion® by fluoro-modified montmorillonite," *Solid State Ionics*, vol. 177, 1137–1144, 2006.
- [12] S. M. J. Zaidi, "Preparation and characterization of composite membranes using blends of SPEEK/PBI with boron phosphate," *Electrochim. Acta*, vol. 50, pp. 4771-4777, 2005.
- [13] L. Du, X. Yan, G. He, X. Wu, Z. Hu and Y. Wang, "SPEEK proton exchange membranes modified with silica sulfuric acid nanoparticles," *Int. J. Hydrogen Energy*, vol. 37, pp. 11853-11861, 2012.
- [14] Z. Q. Jiang, X. S. Zhao and A. Manthiram, "Sulfonated poly(ether ether ketone) membranes with sulfonated graphene oxide fillers for direct methanol fuel cells," *Int. J. Hydrogen Energy*, vol. 38, pp. 5875-5884, 2013.
- [15] M. M. Hasani-Sadrabadi, S. H. Emami, R. Ghaffarian, and H. Moaddel, "Nanocomposite membranes made from sulfonated poly(ether ether ketone) and montmorillonite clay for fuel cell applications," *Energy Fuels*, vol. 22, pp. 2539-2542, 2008.
- [16] Y. S. Kim, F. Wang, M. Hickner, T. A. Zawodzinski, and J. E. McGrath, "Fabrication and characterization of heteropolyacid (H<sub>3</sub>PW<sub>12</sub>O<sub>40</sub>)/directly polymerized sulfonated poly(arylene ether sulfone) copolymer composite membranes for higher temperature fuel cell applications," *J. Membr. Sci.*, vol. 212, pp. 263-282, 2003.
- [17] C. H. Lee, K. A. Min, H. B. Park, Y. T. Hong, B. O. Jung, and Y. M. Lee, "Sulfonated poly(arylene ether sulfone)–silica nanocomposite membrane for direct methanol fuel cell (DMFC)," *J. Membr. Sci.*, vol. 303, pp. 258-266, 2007.
- [18] S. Wen, C. Gong, W. C. Tsen, Y. C. Shu, and F. C. Tsai, "Sulfonated poly(ether sulfone) (SPES)/boron phosphate (BPO<sub>4</sub>) composite membranes for high-temperature proton-exchange membrane fuel cells," *Int. J. Hydrogen Energy*, vol. 34, pp. 8982-8991, 2009.
- [19] D. J. Kim, H. Y. Hwang, S. Y. Nam, and Y. T. Hong, "Characterization of a composite membrane based on SPAES/sulfonated montmorillonite for DMFC application," *Macromol. Res.*, vol. 20, pp. 21-29, 2012.
- [20] Z. Hu, G. He, S. Gu, Y. Liu and X. Wu, "Montmorillonite-Reinforced Sulfonated Poly(phthalazinone ether sulfone ketone) Nanocomposite Proton Exchange Membranes for Direct Methanol Fuel Cells," *J. Appl. Polym. Sci.*, vol. 131, p. 39852, 2014.
- [21] Y. Daiko, H. Sakamoto, K. Katagiri, H. Muto, M. Sakai, and A. Matsuda, "Deposition of ultrathin Nafion layers on sol–gel-derived phenylsilsesquioxane particles via layer-by-layer assembly fuel cells and energy conversion," *J. Electrochem. Soc.*, vol. 155, pp. B479-B482, 2008.
- [22] G. Alberti, M. Casciola, U. Costantino, G. Levi, and G. Ricciardi, "On the mechanism of diffusion and ionic transport in crystalline insoluble acid salts of tetravalent metals. I. Electrical conductance of zirconium bis(monohydrogen ortho-phosphate) monohydrate with a layered structure," *J. Inorg. Nucl. Chem.*, vol. 40, pp. 533-537, 1978.
- [23] Y. Kawakami and M. Miyayama, "Proton conducting properties of layered metal phosphate hydrates," *Key Eng. Mater.*, vol. 320, pp. 267-270, 2006.



- [24] Y. Kozawa, S. Suzuki, and M. Miyayama, "Proton conducting properties of sulfonated poly(etheretherketone) composite membranes with layered tin phosphate hydrates at intermediate temperatures fuel cells and energy conversion," *J. Electrochem. Soc.*, vol. 156, pp. B1401-B1405, 2009.
- [25] D. Yoshimune, S. Sugata, S. Suzuki, and M. Miyayama, "Proton conduction in composite membranes of sulfonated hydrocarbon electrolyte and layered tin phosphate hydrates fuel cells and energy conversion," *J. Electrochem. Soc.*, vol. 159, pp. B91-B95, 2012.
- [26] D. M. Kaschak, S. A. Johnson, D. E. Hooks, H. N. Kim, M. D. Ward, and T. E. Mallouk, "Chemistry on the edge: A microscopic analysis of the intercalation, exfoliation, edge functionalization, and monolayer surface tiling reactions of  $\alpha$ -zirconium phosphate," *J. Am. Chem. Soc.*, vol. 120, pp. 10887-10894, 1998.
- [27] T. Sasaki and M. Watanabe, "Osmotic swelling to exfoliation. Exceptionally high degrees of hydration of a layered titanate," *J. Am. Chem. Soc.*, vol. 120, pp. 4682-4689, 1998.
- [28] L. Wang, Y. Omomo, N. Sakai, K. Fukuda, and I. Nakai, et al., "Fabrication and characterization of multilayer ultrathin films of exfoliated  $\text{MnO}_2$  nanosheets and polycations," *Chem. Mater.*, vol. 15, pp. 2873-2878, 2003.
- [29] K. Nakamura, Y. Oaki and H. Imai, "Monolayered Nanodots of Transition Metal Oxides," *J. Am. Chem. Soc.*, vol. 135, pp. 4501-4508, 2013.
- [30] D. Marani, A. D'Epifanio, E. Traversa, M. Miyayama, and S. Licocchia, "Titania nanosheets (TNS)/sulfonated poly ether ether ketone (SPEEK) nanocomposite proton exchange membranes for fuel cells," *Chem. Mater.*, vol. 22, pp. 1126-1133, 2009.
- [31] Y. Kozawa, S. Suzuki, M. Miyayama, T. Okumiya, and E. Traversa, "Proton conducting membranes composed of sulfonated poly(etheretherketone) and zirconium phosphate nanosheets for fuel cell applications," *Solid State Ionics*, vol. 181, pp. 348-353, 2010.
- [32] S. Sugata, S. Suzuki, M. Miyayama, E. Traversa, and S. Licocchia, "Effects of tin phosphate nanosheet addition on proton-conducting properties of sulfonated poly(ether sulfone) membranes," *Solid State Ionics*, vol. 228, pp. 8-13, 2012.
- [33] G. Alberti, E. Giontella, and S. Murcia-Mascaos, "Mechanism of the formation of organic derivatives of  $\gamma$ -zirconium phosphate by to-potactic reactions with phosphonic acids in water and water-acetone media," *Inorg. Chem.*, vol. 36, pp. 2844-2849, 1997.
- [34] S. Yamanaka and M. Hattori, "Exchange reaction between  $\text{HPO}_4^{2-}$  and  $\text{C}_6\text{H}_5\text{OPO}_3^{2-}$  in a heterogeneous system with  $\gamma$ -zirconium phosphate,  $\text{Zr}(\text{HPO}_4)_2 \cdot 2\text{H}_2\text{O}$ ," *Chem. Lett.*, vol. 8, pp. 1073-1076, 1979.
- [35] S. Yamanaka, K. Sakamoto, and M. Hattori, "Mechanism for the heterogeneous exchange of the interlayer phosphate groups of  $\gamma$ -zirconium phosphate with phenyl phosphate groups," *J. Phys. Chem.*, vol. 88, pp. 2067-2070, 1984.
- [36] G. Alberti, U. Costantino, S. Allulli, and N. Tomassini, "Crystalline  $\text{Zr}(\text{R-PO}_3)_2$  and  $\text{Zr}(\text{R-OPO}_3)_2$  compounds (R = organic radical): A new class of materials having layered structure of the zirconium phosphate type," *J. Inorg. Nucl. Chem.*, vol. 40, pp. 1113-1117, 1978.
- [37] M. B. Dines and P. M. Digiacomo, "Derivatized lamellar phosphates and phosphonates of M(IV) ions," *Inorg. Chem.*, vol. 20, pp. 92-97, 1981.
- [38] G. Alberti and M. Casciola, "Layered metalIV phosphonates, a large class of inorgano-organic proton conductors," *Solid State Ionics*, vol. 97, pp. 177-186, 1997.
- [39] G. Alberti, M. Casciola, A. Donnadio, P. Piaggio, M. Pica, and M. Sisani, "Preparation and characterisation of  $\alpha$ -layered zirconium phosphate sulfophenylphosphonates with variable concentration of sulfonic groups," *Solid State Ionics*, vol. 176, pp. 2893-2898, 2005.
- [40] F. Wang, M. Hickner, Q. Ji, W. Harrison, J. Mecham, T. A. Zawodzinski, and J. E. McGrath, "Synthesis of highly sulfonated poly(arylene ether sulfone) random (statistical) copolymers via direct polymerization," *Macromol. Symp.*, vol. 175, pp. 387-396, 2001.
- [41] F. Wang, M. Hickner, Y. S. Kim, T. A. Zawodzinski, and J. E. McGrath, "Direct polymerization of sulfonated poly(arylene ether sulfone) random (statistical) copolymers: Candidates for new proton exchange membranes," *J. Membr. Sci.*, vol. 197, pp. 231-242, 2002.
- [42] E. Montoneri, M. C. Gallazzi, and M. Grassi, "Organosulphur phosphorus acid compounds. Part 1. m-Sulphophenylphosphonic acid," *J. Chem. Soc., Dalton Trans.*, pp. 1819-1823, 1989.
- [43] H. G. M. Edwards, D. R. Brown, J. R. Dale, and S. Plant, "Raman spectroscopic studies of acid dissociation in sulfonated polystyrene resins," *J. Mol. Struct.*, vol. 595, pp. 111-125, 2001.
- [44] D. Whittington and J. R. Millar, "Infra-red absorption spectra of ion-exchange resins," *J. Appl. Chem. (London, U. K.)*, vol. 18, pp. 122-128, 1968.
- [45] P. Krishnan, J. S. Park, and C. S. Kim, "Preparation of proton-conducting sulfonated poly(ether ether ketone)/boron phosphate composite membranes by an in situ sol-gel process," *J. Membr. Sci.*, vol. 279, pp. 220-229, 2006.
- [46] M. Cappadonia, J. W. Erning, S. M. Saberi Niaki, and U. Stimming, "Conductance of Nafion 117 membranes as a function of temperature and water content," *Solid State Ionics*, vol. 77, pp. 65-69, 1995.